

## SUPPLEMENTAL TABLE AND FIGURE LEGENDS

**Supplemental Table 1. Genes expression clusters.** Table listing the genes in each of the 14 expression clusters in Figure 1A.

**Supplemental Table 2. Putative transcription factors regulating genes in each cluster.** For each cluster, the top enriched transcription factors, source of ChIP-seq data [1-3], and enrichment statistics as calculated by Enrichr [4] are provided.

**Supplemental Table 3. Highly connected nodes within Cluster 1 network.** The top 5 nodes based on network centrality (betweenness) as calculated by esyN [5].

**Supplemental Table 4. Putative NRF2 target genes in Cluster 1.** NRF2 target genes in Cluster 1, as called by Enrichr [4].

**Supplemental Figure S1. TBOOH treatment increases *HIF1A* mRNA expression in multiple cell types.** (A) *HIF1A* expression in HepG2 cells treated for 8 hours with vehicle control or TBOOH. Gene expression values were measured by quantitative reverse transcription PCR, and normalized relative to *ACTB* expression. (B) Same as (A) only for MCF7 breast cancer cell. (C) Same as (A) only for MDA-MB-231 breast cancer cells. Gene expression changes were measured after 8 hours of TBOOH exposure and, to avoid confounding cell death gene expression signatures, TBOOH treatments for each cell line were based on a concentration that resulted in 80% cell viability after 24 hours (24hr EC<sub>80</sub>). The 24hr EC<sub>80</sub> for HepG2 was 300µM, for MCF7 was 80µM, and for MDA-MB-231 was 100µM. Asterisks represent p-values for TBOOH versus vehicle for each cell type (\*\*p ≤ 0.001; \*\*p ≤ 0.01; \*p ≤ 0.05, Welch's t-test).

**Supplemental Figure S2. An NRF2 binding site at the *HIF1A* locus.** (A) An NRF2 ChIP-seq peak at the human *HIF1A* locus. ChIP-seq data are the same as described in Figure 3A, only zoomed out to show more of the genomic region around *HIF1A*. The center column represents compiled topologically associated domain (TAD) boundaries from high-throughput chromosome conformation capture (Hi-C) datasets [6, 7]. A region that is called as a TAD in eight out of eight profiled cell types is highlighted with a box. Overall, four genes have transcription start sites that fall within this TAD: *HIF1A* and three noncoding RNAs (*FLJ22447* and the *HIF1A* antisense RNAs *HIF1A-AS1* and *HIF1A-AS2*). (B) Zoomed in ChIP-seq data from A, equivalent to region presented in Figure 3A. The “Chromatin State” track summarizes chromatin state calls across 127 human tissues and cell types by the Roadmap Epigenomics Project [8]. The height of the color is proportional to the number of cell/tissue types where given chromatin state is called; for example, the prominent red peak near the start of the *HIF1A* gene represents a region that is called as an active transcription start site (TSS) in almost all cells or tissues. The NRF2 ChIP-seq peak overlaps a prominent enhancer (yellow) region at this locus.

**Supplemental Figure S3. Inducible ARE binding at the *HIF1A* locus.** (A) NRF2 ChIP-seq fold enrichment values for the ARE-containing peak at the human *HIF1A* locus. Fold enrichment values from vehicle/control treated lymphoblastoid cells (DMSO; DMSO = dimethylsulfoxide) and from sulforaphane treated lymphoblastoid cells. As in Figure 3A, data are from Chorley et al. ChIP-seq fold enrichment values are calculated relative to negative controls (merged mock and input samples) from the same cells. Fold enrichment values were calculated using MACS2. (B) Same as (A), only for ChIP-seq enrichment significance [-log<sub>10</sub>(q-value)] as calculated by

**MACS2. (C)** Electrophoretic mobility shift assay (EMSA) using either the ARE from the *NQO1* promoter or the ARE from the *HIF1A* enhancer as a labeled probe, as indicated. Each labeled probe was incubated with increasing amounts of nuclear protein lysate from MCF7 cells that had either been treated with 0.1% ethanol (EtOH; vehicle/control treatment) or with 10µM menadione for 8 hours. Lanes marked with “Ø” contain no protein (labeled probe only) and all other lanes have increasing amounts (0.5 µg, 1 µg, or 2 µg) of the indicated lysate. Binding levels at the uppermost band (Band 1) for each probe are increased approximately 1.5-fold for both the *NQO1* and *HIF1A* probe ( $1.49 \pm 0.25$ , and  $1.57 \pm 0.10$ , respectively). Binding levels do not increase for Band 2, so Band 1 is the ROS-responsive band in MCF7 lysates. Probe sequences are the same as in Figure 3C, however, an IRDye labeled *HIF1A* ARE probe was used in this experiment. **(D)** Quantitation of binding levels from (C). For each lane, Band 1 levels were normalized relative to Band 2, and MCF7+menadione binding signals were compared to MCF7+EtOH binding signals for the corresponding lysate concentration. The bar graph represents average of these comparisons for each probe ( $\pm$  standard deviation); values over 1 represent a stronger binding signal in lysates from menadione treated cells.

## SUPPLEMENTAL REFERENCES

- [1] Lachmann, A.; Xu, H.; Krishnan, J.; Berger, S. I.; Mazloom, A. R.; Ma'ayan, A. ChEA: transcription factor regulation inferred from integrating genome-wide ChIP-X experiments. *Bioinformatics* **26**:2438-2444; 2010.
- [2] Boyle, A. P.; Araya, C. L.; Brdlik, C.; Cayting, P.; Cheng, C.; Cheng, Y.; Gardner, K.; Hillier, L. W.; Janette, J.; Jiang, L.; Kasper, D.; Kawli, T.; Kheradpour, P.; Kundaje, A.; Li, J. J.; Ma, L.; Niu, W.; Rehm, E. J.; Rozowsky, J.; Slattery, M.; Spokony, R.; Terrell, R.; Vafeados, D.; Wang, D.; Weisdepp, P.; Wu, Y. C.; Xie, D.; Yan, K. K.; Feingold, E. A.; Good, P. J.; Pazin, M. J.; Huang, H.; Bickel, P. J.; Brenner, S. E.; Reinke, V.; Waterston, R. H.; Gerstein, M.; White, K. P.; Kellis, M.; Snyder, M. Comparative analysis of regulatory information and circuits across distant species. *Nature* **512**:453-456; 2014.
- [3] Sloan, C. A.; Chan, E. T.; Davidson, J. M.; Malladi, V. S.; Stratton, J. S.; Hitz, B. C.; Gabdank, I.; Narayanan, A. K.; Ho, M.; Lee, B. T.; Rowe, L. D.; Dreszer, T. R.; Roe, G.; Poduturi, N. R.; Tanaka, F.; Hong, E. L.; Cherry, J. M. ENCODE data at the ENCODE portal. *Nucleic acids research* **44**:D726-732; 2016.
- [4] Kuleshov, M. V.; Jones, M. R.; Rouillard, A. D.; Fernandez, N. F.; Duan, Q.; Wang, Z.; Koplev, S.; Jenkins, S. L.; Jagodnik, K. M.; Lachmann, A.; McDermott, M. G.; Monteiro, C. D.; Gundersen, G. W.; Ma'ayan, A. Enrichr: a comprehensive gene set enrichment analysis web server 2016 update. *Nucleic acids research* **44**:W90-97; 2016.
- [5] Bean, D. M.; Heimbach, J.; Ficarella, L.; Micklem, G.; Oliver, S. G.; Favrin, G. esyN: network building, sharing and publishing. *PLoS one* **9**:e106035; 2014.
- [6] Rao, S. S.; Huntley, M. H.; Durand, N. C.; Stamenova, E. K.; Bochkov, I. D.; Robinson, J. T.; Sanborn, A. L.; Machol, I.; Omer, A. D.; Lander, E. S.; Aiden, E. L. A 3D map of the human genome at kilobase resolution reveals principles of chromatin looping. *Cell* **159**:1665-1680; 2014.
- [7] Durand, N. C.; Robinson, J. T.; Shamim, M. S.; Machol, I.; Mesirov, J. P.; Lander, E. S.; Aiden, E. L. Juicebox Provides a Visualization System for Hi-C Contact Maps with Unlimited Zoom. *Cell systems* **3**:99-101; 2016.
- [8] Kundaje, A.; Meuleman, W.; Ernst, J.; Bilenky, M.; Yen, A.; Heravi-Moussavi, A.; Kheradpour, P.; Zhang, Z.; Wang, J.; Ziller, M. J.; Amin, V.; Whitaker, J. W.; Schultz, M. D.; Ward, L. D.; Sarkar, A.; Quon, G.; Sandstrom, R. S.; Eaton, M. L.; Wu, Y. C.; Pfennig, A. R.; Wang, X.; Claussnitzer, M.; Liu, Y.; Coarfa, C.; Harris, R. A.; Shores, N.; Epstein, C. B.; Gjoneska, E.; Leung, D.; Xie, W.; Hawkins, R. D.; Lister, R.; Hong, C.; Gascard, P.; Mungall, A. J.; Moore, R.; Chuah, E.; Tam, A.; Canfield, T. K.; Hansen, R. S.; Kaul, R.; Sabo, P. J.; Bansal, M. S.; Carles, A.; Dixon, J. R.; Farh, K. H.; Feizi, S.; Karlic, R.; Kim, A. R.; Kulkarni, A.; Li, D.; Lowdon, R.; Elliott, G.; Mercer, T. R.; Neph, S. J.; Onuchic, V.; Polak, P.; Rajagopal, N.; Ray, P.; Sallari, R. C.; Siebenthal, K. T.; Sinnott-Armstrong, N. A.; Stevens, M.; Thurman, R. E.; Wu, J.; Zhang, B.; Zhou, X.; Beaudet, A. E.; Boyer, L. A.; De Jager, P. L.; Farnham, P. J.; Fisher, S. J.; Haussler, D.; Jones, S. J.; Li, W.; Marra, M. A.; McManus, M. T.; Sunyaev, S.; Thomson, J. A.; Tlsty, T. D.; Tsai, L. H.; Wang, W.; Waterland, R. A.; Zhang, M. Q.; Chadwick, L. H.; Bernstein, B. E.; Costello, J. F.; Ecker, J. R.; Hirst, M.; Meissner, A.; Milosavljevic, A.; Ren, B.; Stamatoyannopoulos, J. A.; Wang, T.; Kellis, M. Integrative analysis of 111 reference human epigenomes. *Nature* **518**:317-330; 2015.

**Supplemental Table 2**

Cluster	Transcription Factor	Source	P-value	Adj P-value	Z-score	Combined score
1	NFE2L2	CHEA	3.15E-11	3.22E-09	-1.64	39.62
	ZBTB7A	ENCODE	2.89E-08	1.47E-06	-1.62	28.16
	UBTF	ENCODE	1.18E-07	4.03E-06	-1.6	25.5
2	RUNX1	CHEA	7.09E-06	0.00053	-1.67	19.78
	E2F6	ENCODE	1.15E-05	0.00053	-1.63	18.51
	NFE2L2	CHEA	1.53E-05	0.00053	-1.57	17.37
3	--	--	--	--	--	--
4	UBTF	ENCODE	1.77E-10	1.70E-08	-1.67	37.55
5	--	--	--	--	--	--
6	E2F4	ENCODE	8.97E-31	8.88E-29	-1.77	122.45
	SIN3A	ENCODE	1.90E-07	7.02E-06	-1.73	26.78
	NFYB	ENCODE	2.13E-07	7.02E-06	-1.62	24.87
7	--	--	--	--	--	--
8	--	--	--	--	--	--
9	TP53	CHEA	1.27E-05	0.000701	-1.68	18.92
10	HNF4A	ENCODE	9.05E-29	9.42E-27	-1.73	111.52
	E2F4	ENCODE	1.63E-17	8.48E-16	-1.73	67
	FOXM1	ENCODE	1.36E-15	4.70E-14	-1.79	61.39
11	CEBDP	ENCODE	9.36E-06	0.000852	-1.73	20.06
12	TCF3	ENCODE	1.5E-06	0.000138	-1.63	21.91
13	--	--	--	--	--	--
14	E2F4	ENCODE	3.85E-06	0.000358	-1.77	22.07

**Supplemental Table 3**

Gene	Node Betweenness Score
SQSTM1	1
UBE2D1	0.91
CBL	0.68
TRIM21	0.66
HIF1A	0.53

**Supplemental Table 4**

Putative NRF2 Targets in Cluster 1					
ABCC5	GCLC	KLF5	OSGIN1	SLC25A30	TMEFF1
ASF1A	GCLM	KLHL21	PAWR	SLC40A1	TMEM159
C16ORF72	GPCPD1	KRAS	PDLIM3	SLC7A11	TNFRSF1A
C5ORF30	GRB10	LMCD1	PIK3CD	SQSTM1	TRIB1
DLX2	GRK5	LRP8	PXDC1	SRXN1	TSKU
DUSP4	HMOX1	MAFF	RGMB	ST3GAL4	TUBE1
F3	IGFBP3	MAFG	RGS10	STC2	ZNF330
FBLIM1	JAG1	MEGF9	RICTOR	STIM2	ZYX
FOPNL	KLF4	MSANTD3	SGK223	TMC7	

**Figure S1**

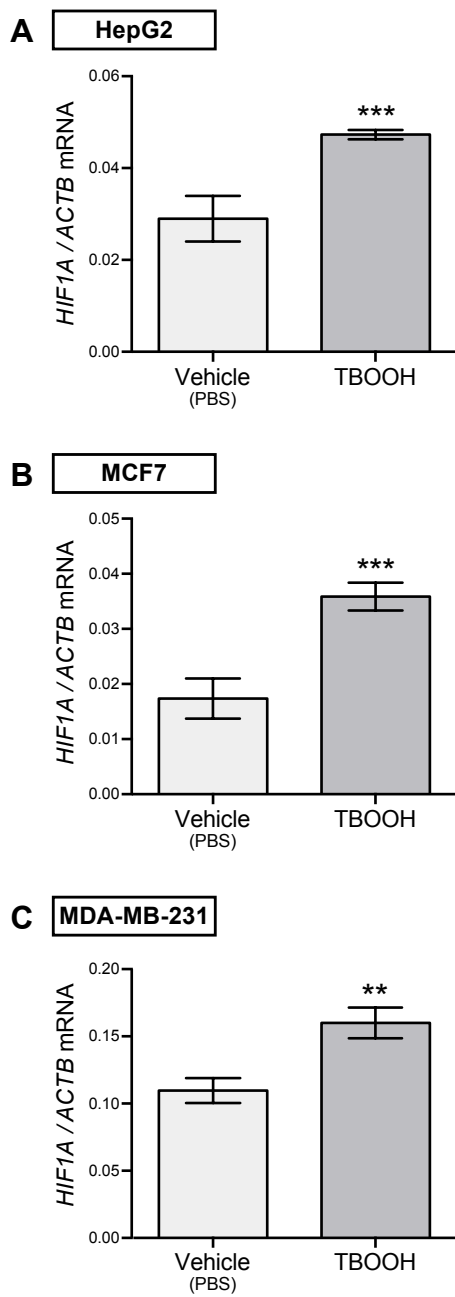


**Figure S2**

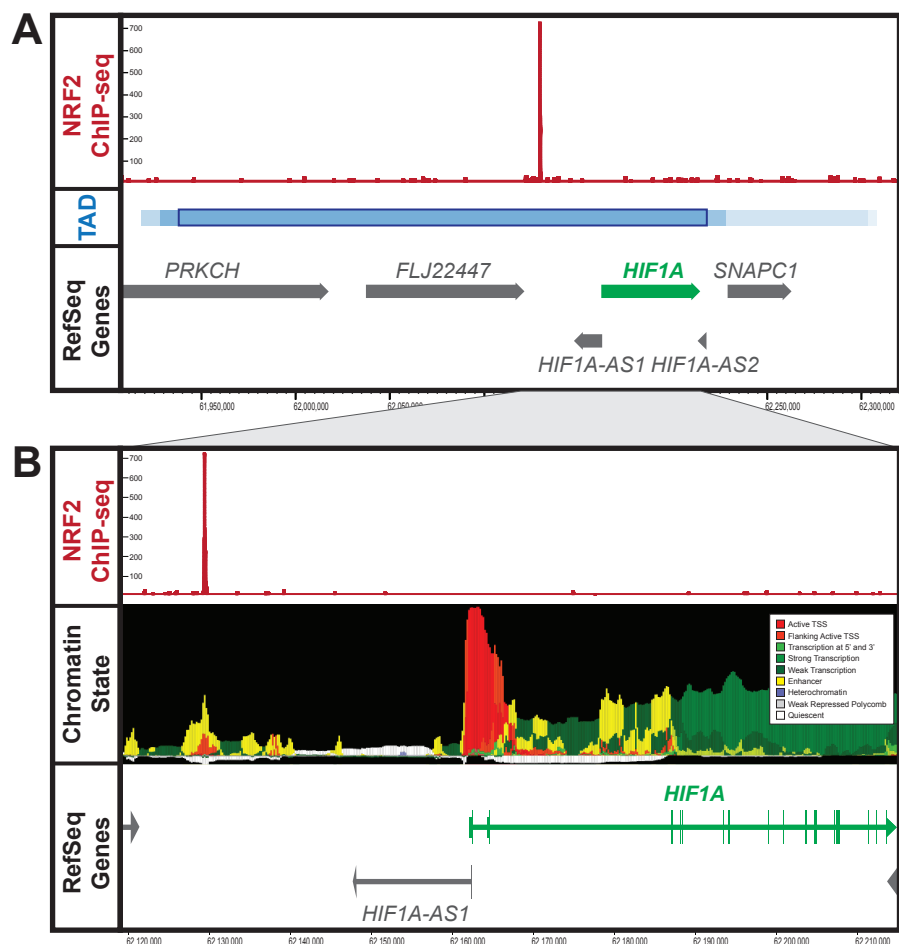


**Figure S3**

